Optically detected magnetophonon resonances in *n*-Ge in tilted magnetic fields

Sang Chil Lee,[1] Hyung Soo Ahn,[2] Dong Shik Kang,[1] Seong Oh Lee,[3] and Suck Whan Kim[3]
[1]*Department of Physics, Cheju National University, Cheju 690–756, Korea*
[2]*Department of Applied Physics, Korea Maritime University, Pusan 606-791, Korea*
[3]*Department of Physics, Andong National University, Andong 760–749, Korea*
(Received 16 October 2002; published 31 March 2003)

We investigate the influence of the angular dependence of optically detected magnetophonon resonance (ODMPR) in *n*-type germanium in a tilted magnetic field. With the ODMPR conditions, qualitative features of the ODMPR effects are investigated according to the incident photon frequency, the strength of the magnetic field, the temperature, and the difference of Landau level indices as a function of the tilt angle to the applied magnetic field in the quantum limit condition, in which $\hbar\omega_c \gg k_BT$ is satisfied. In particular, anomalous behaviors of the ODMPR line shape, such as the splitting and the shift of ODMPR peaks, are discussed in detail.

DOI: 10.1103/PhysRevB.67.115342 PACS number(s): 73.21.−b, 73.40.−c, 72.20.Dp

The optically detected magnetophonon resonance (ODMPR) allows one to make quantitative measurements of the scattering strength for specific Landau levels, and yields direct information on the nature of the electron-phonon interaction in semiconductors.[1–8] The purpose of the present work is to investigate the angular dependence of the optically detected magnetophonon resonance effects on the magnetoconductivity of *n*-Ge in the tilted magnetic fields obtained by using the Mori-type projection operator technique,[9] and to investigate the features of optically detected magnetophonon resonance effects in magnetoconductivity as a function of the incident photon frequency, the strength of magnetic field, the difference of Landau level indices, and the temperature in such materials.

Consider a system of many noninteracting electrons N_e in interaction with phonons, initially in equilibrium with a temperature T. Then, in the presence of the static magnetic field tilted with an angle of θ from the z axis chosen to be parallel to the principal axis of an ellipsoidal energy surface, $\mathbf{B}=B(\sin\theta,0,\cos\theta)$, with the Landau guage of vector potential $\mathbf{A}=B(-y\cos\theta,0,y\sin\theta)$, one-electron normalized eigenfuncitons $F_\lambda(\mathbf{r})$, and eigenvalues E_λ in the conduction band are given, respectively, by

$$F_\lambda(\mathbf{r})=\frac{1}{\sqrt{L_xL_z}}\phi_N(y-y_\lambda)\exp(ik_xx+ik_zz), \tag{1}$$

$$E_\lambda=E_N(k_x,k_z)=(N+1/2)\hbar\omega_s+\hbar^2(\mathbf{k}\cdot\mathbf{B}/B)^2/2m_B, \tag{2}$$

where $|\lambda\rangle$ means the Landau states $|N,\mathbf{k}\rangle$ in the conduction band and $N(=0,1,2,\ldots)$ is the Landau-level index. $\phi_N(y)$ are the eigenfunctions of the simple harmonic oscillator with $y_\lambda=(m_tk_z\sin\theta-m_lk_x\cos\theta)\hbar/eBm_B$, and L_x and L_z are, respectively, the x- and z-directional normalization lengths. k_x and k_z are, respectively, the wave vector component of the electron in the x and z direction, $\omega_s(=eB/m_s)$ is the cyclotron frequency in the conduction band, and m_B is the effective mass in the magnetic field direction with $m_B=m_l\cos^2\theta+m_t\sin^2\theta$. Here $1/m_s^2=\cos^2\theta/m_t^2+\sin^2\theta/(m_tm_l)$.

When a linearly polarized electromagnetic wave of amplitude $E=(0,E\cos\omega t,0)$ with frequency ω is applied along the z axis, the absorption power delivered to the system is $P=E^2\,\mathrm{Re}[\bar{\sigma}_{yy}(\bar{\omega})]/2$ for the Faraday configuration $(E\perp B)$,[9,10] where Re means "the real part of" $\bar{\omega}=\omega-i\delta$ $(\delta\to0^+)$, $\bar{\sigma}_{yy}(\bar{\omega})\equiv[\sigma_{yy}(\bar{\omega})+\sigma_{yy}(-\bar{\omega})]/2$ and $\sigma_{yy}(\bar{\omega})$ [or $\sigma_{yy}(-\bar{\omega})$] is the complex optical conductivity corresponding to the right (or left) circularly polarized wave, which can be expressed in the linear-response theory as[9,10]

$$\sigma_{yy}(\bar{\omega})=\frac{\hbar}{i\Omega}\sum_{\lambda',\lambda}\frac{f(E_{\lambda'})-f(E_\lambda)}{E_{\lambda'}-E_\lambda}\times\frac{|j_{y\lambda'\lambda}|^2}{\hbar\bar{\omega}-E_{\lambda'}+E_\lambda-i\hbar\tilde{\Sigma}_{0\lambda'\lambda}(\bar{\omega})}, \tag{3}$$

where Ω represents the volume of the system, j_y is the y component of the single-electron current operator, $f(E_\lambda)$ is a Fermi-Dirac distribution function, and the quantity $i\hbar\tilde{\Sigma}_{0\lambda'\lambda}(\bar{\omega})$ means the line shape function. Therefore, the real parts and the imaginary parts of $i\hbar\tilde{\Sigma}_{0\lambda'\lambda}(\bar{\omega})$ are, respectively, defined by the lineshift terms $[\hbar\tilde{\nabla}_{0\lambda'\lambda}(\bar{\omega})]$ and the linewidth terms $[i\hbar\tilde{\Gamma}_{0\lambda'\lambda}(\bar{\omega})]$, for the transition arising from the resonant absorption or emission of a single photon of frequency ω and of a single phonon of frequency $\omega_{\mathbf{q}}$ between states $|\lambda\rangle$ and $|\lambda'\rangle$.

To obtain the magnetoconductivity $\sigma_{yy}(\bar{\omega})$ of Eq. (3) for the nondegenerate limit and the quantum limit $(\hbar\omega_c\gg k_BT)$, we use the matrix elements of the y-component single-electron current operator given by

$$|\langle Nk_xk_z|j_y|N'k_x'k_z'\rangle|^2=\frac{e^2m_s\hbar\omega_s}{m_t^2}[(N+1)\delta_{N+1N'}+N\delta_{N-1N'}]\delta_{k_x,k_x'}\delta_{k_z,k_z'}. \tag{4}$$

The angular dependent magnetoconductivity is directly proportional to the matrix element with respect to the current operator in Eq. (4). We also replace summations with respect to k_x and k_z of $\Sigma_{\lambda(=N,k_x,k_z)}$ in Eq. (3) by the relation:[6]

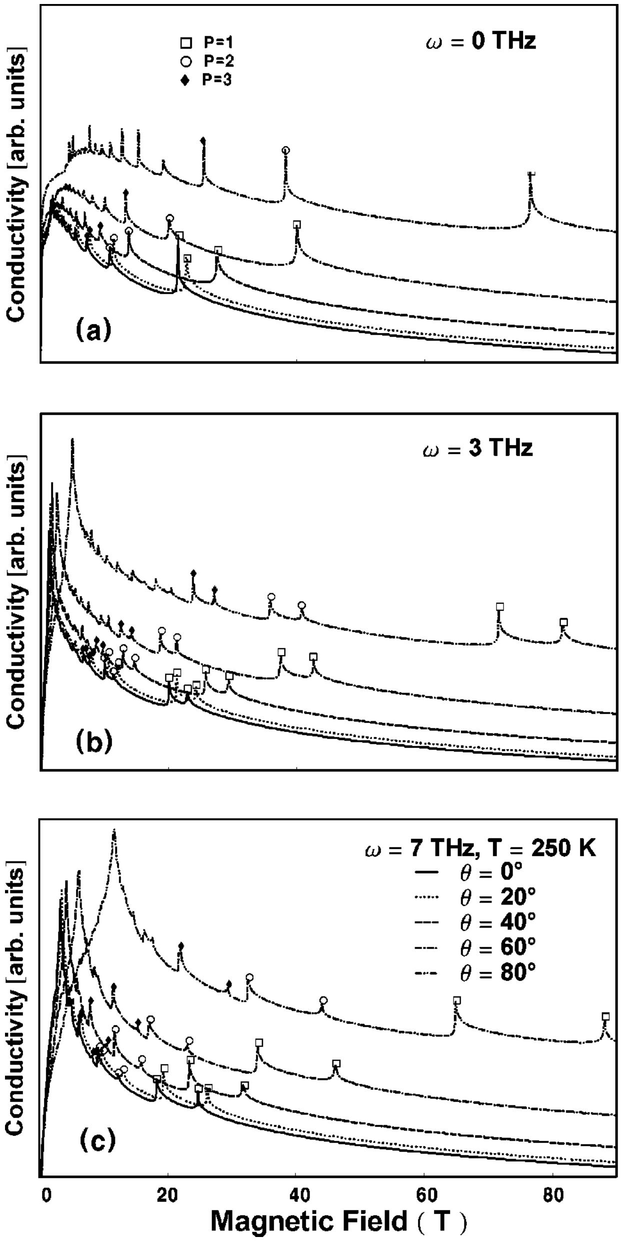

FIG. 1. Spectral line shapes of the magnetoconductivity $[\overline{\sigma_{yy}}(\overline{\omega})]$ as a function of the applied magnetic field for *n*-Ge at $T=250$ K as a function of magnetic field B for the various tilt angles θ of the tilted magnetic field in cases of $\omega=0$, 3, and 7 THz.

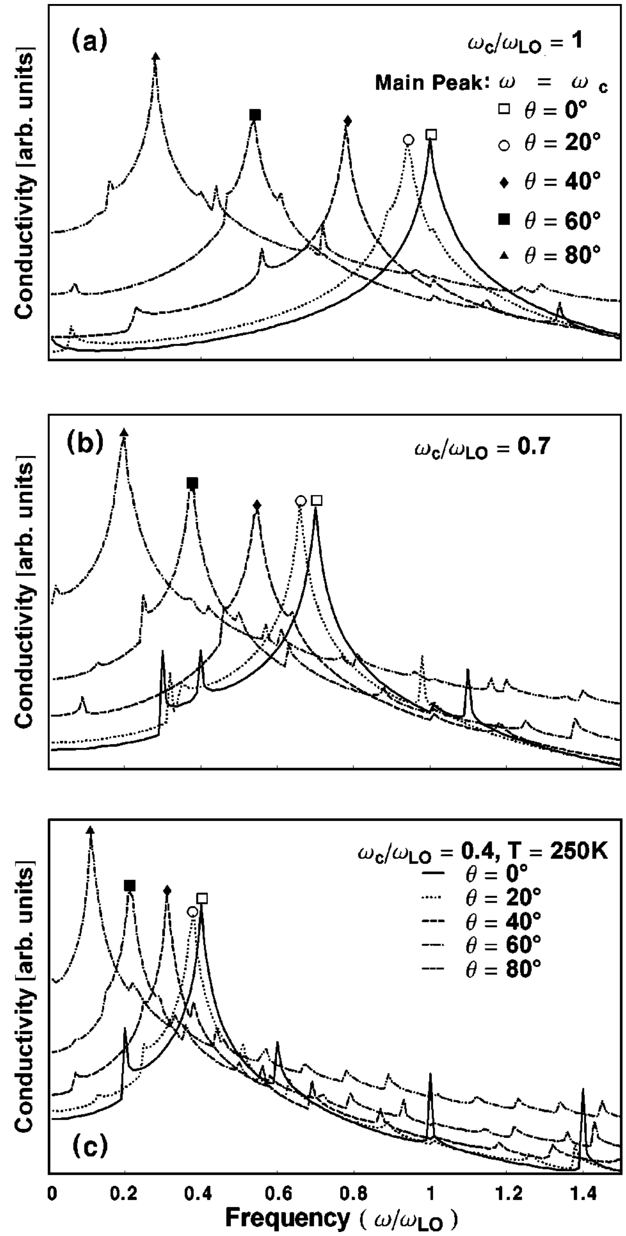

FIG. 2. Magnetic field strength dependence of the magnetoconductivity $[\overline{\sigma_{yy}}(\overline{\omega})]$ as a function of the ratio between the incident photon frequency and the phonon frequency, ω/ω_{LO}, for various tilt angles θ at $T=250$ K in cases of $\omega_c/\omega_{LO}=1.0$, 0.7, and 0.3, respectively. Here ω_c means eB/m_t.

$\Sigma_{k_x,k_z}(\cdots)=L_xL_z/(4\pi^2)\int\int_{1stBZ}dk_xdk_z(\cdots)$ because the ranges of k_x and k_z are, respectively, given within

$$-\frac{eBm_BL_y}{2\hbar m_l\cos\theta}+\frac{m_t}{m_l}k_z\tan\theta<k_x<\frac{eBm_BL_y}{2\hbar m_l\cos\theta}+\frac{m_t}{m_l}k_z\tan\theta$$

and $-\pi/L_z<k_z<\pi/L_z$. In addition, we assume that the f's in Eq. (3) can be replaced by the Boltzmann distribution function for nondegenerate semiconductor,[6] i.e., $f[E_N(k_z)]\approx\exp[\beta(\mu-E_N(k_x,k_z))]$, where $\beta=1/k_BT$, with Boltzmann constant k_B and temperature T, and the chemical potential μ is $1/\beta\ln[\sqrt{\beta/(2\pi m_B)}4\pi^2n_e\hbar^2m_l\cos\theta\sinh[(\beta/2)\hbar\omega_s]/(m_s\omega_sm_B)]$ with the electron density $n_e(=N_e/\Omega)$. Then we obtain the angular dependent magnetoconductivity corresponding to the right circularly polarized wave as

$$\sigma_{yy}(\overline{\omega})=\sqrt{\frac{2\beta e^4\hbar^4n_e^2m_s^2}{\pi m_Bm_l^2m_t^4\cos^2\theta}}e^{-\beta\hbar\omega_s/2}\sinh^2\left(\frac{\beta}{2}\hbar\omega_s\right)\times\sum_N(N+1)e^{-\beta[N+(1/2)]\hbar\omega_s}\int_{-\pi/L_z}^{\pi/L_z}e^{-\beta\hbar^2k_z^2/2m_B}\times\frac{\Gamma_{N+1,k_x,k_z;N,k_x,k_z}(\omega)}{(\hbar\omega-\hbar\omega_s)^2+\Gamma^2_{N+1,k_x,k_z;N,k_x,k_z}(\omega)}dk_z \qquad (5)$$

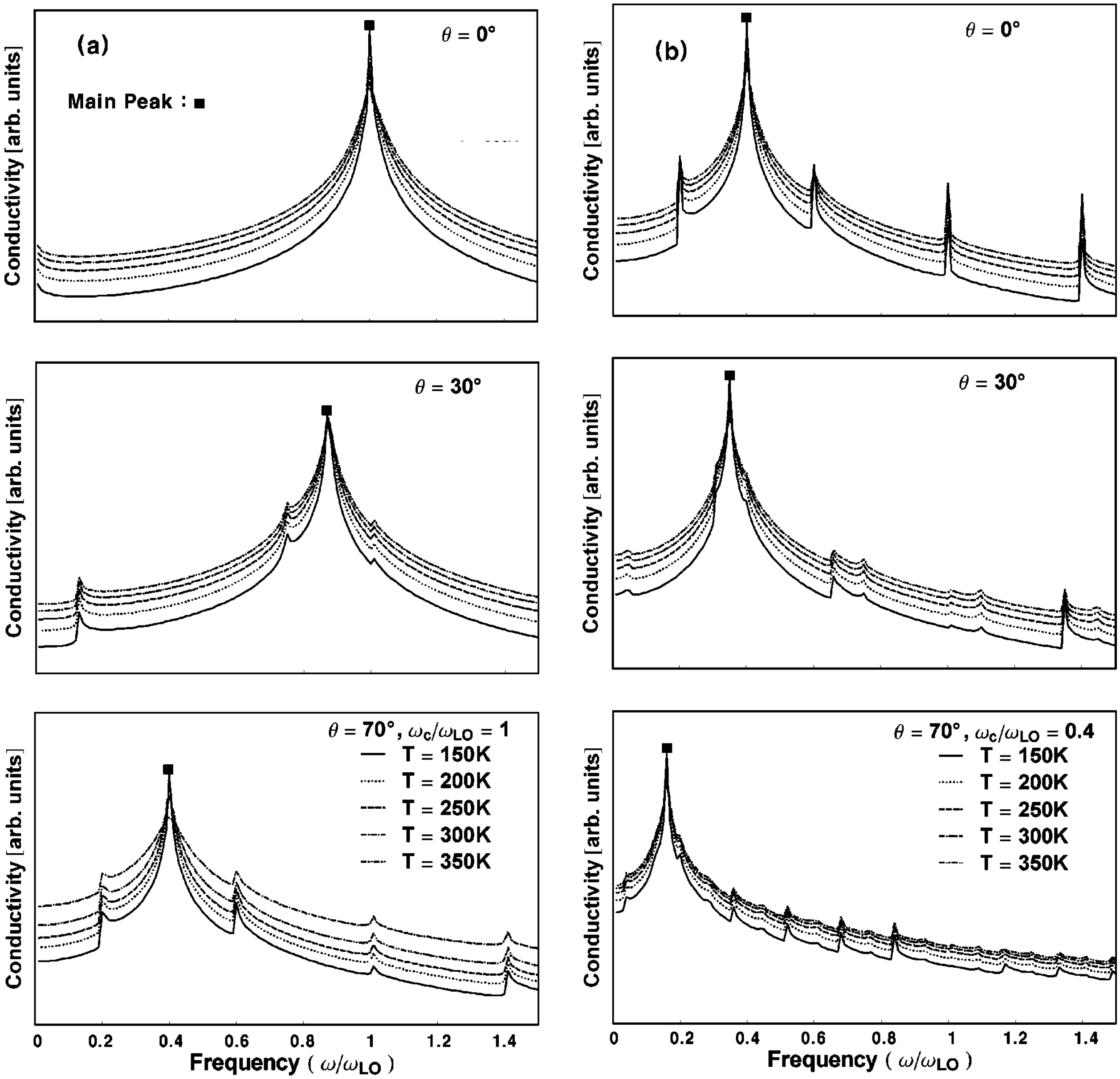

FIG. 3. Magnetic field strength dependence of the magnetoconductivity $[\overline{\sigma_{yy}}(\overline{\omega})]$ as a function of the ratio between the incident photon frequency and the phonon frequency, ω/ω_{LO}, for various temperature in cases of $\theta=0°$, $\theta=30°$, and $\theta=70°$, respectively, for (a) $\omega_c/\omega_{LO}=1.0$ and (b) $\omega_c/\omega_{LO}=0.4$.

for a shift of zero, $\tilde{\nabla}_0 \simeq 0$, in the spectral lineshape.

The relaxation rates $\Gamma(\omega)$ in Eq. (5) associated with the electronic transition between $|N+1,k_x',k_z'\rangle$ and $|N,k_x',k_z'\rangle$ can be expressed for nonpolar optical phonon scattering by

$$\Gamma_{N+1,k_x',k_z';N,k_x',k_z'} = \frac{\sqrt{m_B}D'}{2\sqrt{2}\pi\hbar} \sum_{N'\neq N} \left\{ (n_0+1)\left(\frac{\theta[\Theta_{1-}(k_z')]}{\sqrt{\Theta_{1-}(k_z')}} + \frac{\theta[\Theta_{2+}(k_z')]}{\sqrt{\Theta_{2+}(k_z')}} \right) + n_0 \left(\frac{\theta[\Theta_{1+}(k_z')]}{\sqrt{\Theta_{1+}(k_z')}} + \frac{\theta[\Theta_{2-}(k_z')]}{\sqrt{\Theta_{2-}(k_z')}} \right) \right\}, \tag{6}$$

with

$$\Theta_{1\pm}(k_z') = \hbar\omega + (N-N')\hbar\omega_s + \frac{\hbar^2 k_z'^2}{2m_B^*} \pm \hbar\omega_{LO}, \tag{7}$$

$$\Theta_{2\pm}(k_z') = \hbar\omega + (N'-N-1)\hbar\omega_s - \frac{\hbar^2 k_z'^2}{2m_B^*} \pm \hbar\omega_{LO}, \tag{8}$$

where $n_0=[\exp(\beta\hbar\omega_{LO})-1]^{-1}$ is the phonon distribution function, $\theta(x)$ in Eq. (6) is Heaviside step function by $\theta(x)=1$ for $x\geqslant 0$ and 0 for $x<0$. Here $k_x'=k_x\cos\theta - k_z\sin\theta$, and $k_z'=k_x\sin\theta + k_z\cos\theta$. In order to obtain Eq. (6), we transformed the sum over q_z' into an integral form in

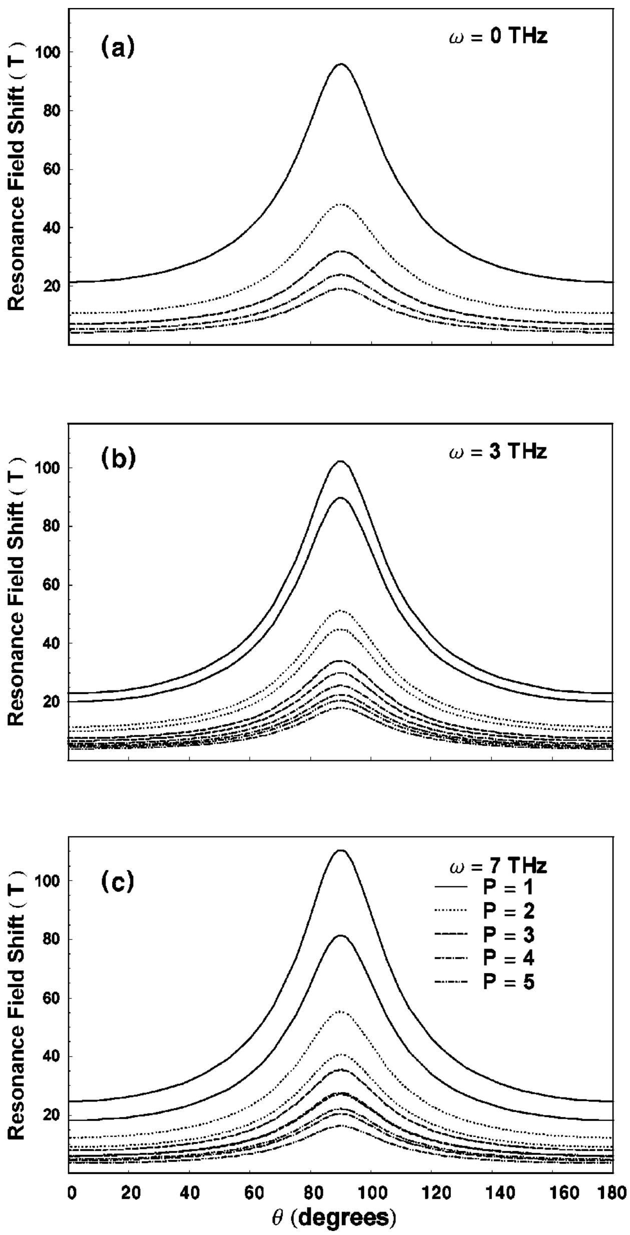

FIG. 4. Shifts of resonant peaks as a function of tilt angle θ of an applied magnetic field for various differences of Landau level indices in cases of $\omega=0$, 3, and 7 THz.

the usual way as $\Sigma_{q_z'}\rightarrow[L_z/(2\pi)]\int_{-\pi/L_z}^{\pi/L_z}dq_z'$ and used the following property of the Dirac delta function: $\delta[f(x)]=\Sigma_i\delta[x-x_i]/|f'(x_i)|$ with x_i being the roots of $f(x)$. From these conditions, the relaxation rates [and hence, the angular dependent magnetoconductivities $\sigma_{yy}(\omega)$ and $\sigma_{yy}(-\omega)$] for the nonpolar LO-phonon scattering show the resonant behaviors at $P\hbar\omega_s\pm\hbar\omega=\hbar\omega_{LO}$ $(P\equiv N'-N=1,2,3,\dots)$. When the ODMPR conditions are satisfied, in the course of scattering events, the electrons in the Landau levels N can make transitions to one of the Landau levels N' by absorbing and/or emitting a photon of energy $\hbar\omega$ during the absorption of a LO phonon of energy $\hbar\omega_{LO}$. Equation (5) is the basic equations for the ODMPR spectral line shape, which enables us to analyze ODMPR effects in semiconductors under the tilted magnetic fields.

We present the numerical results of the angular dependent magnetoconductivity formula $\overline{\sigma_{yy}}(\overline{\omega})$ in Eq. (5). Here, special attention is given to the behavior of the ODMPR line shape, such as the appearance of ODMPR peaks, the angular dependent magnetoconductivity, and the shift of ODMPR peaks. For our numerical results, the parameters of n-Ge are taken[11,12] by effective masses $m_t=0.082m_0$ and $1.64m_0$, with m_0 being the electron rest mass, a LO-phonon energy $\hbar\omega_{LO}=30.3$ meV, the electron density $n_e=4\times10^{24}$ m^{-3}, and the constant of the nonpolar interaction $D'=1.059\times10^{-68}$ kg^2 m^7 s^{-4}. In addition, as many as 21 Landau levels are included in the calculation of the angular dependent magnetoconductivity.

Figures 1(a), 1(b), and 1(c) show the spectral line shapes of the magnetoconductivities for the nonpolar material n-Ge as a function of magnetic field for the various tilt angles θ of the tilted magnetic field B applied to the bulk material in case of $\omega=0$, 3, and 7 THz at $T=250$ K. As shown in Figs. 1(a), 1(b), and 1(c), we can see the following features: (i) Various peaks depending on the P values are observed in the $\overline{\sigma_{yy}}(\overline{\omega})$ at each tilt angle. (ii) As the difference of Landau level indices increases, the MPR $(\omega=0)$ and ODMPR peak positions are shifted to the lower magnetic field region. (iii) The shift of the resonant peaks in the $\overline{\sigma_{yy}}(\overline{\omega})$ is sensitive to the tilt angle θ of the applied magnetic field. The peaks in the magnetoconductivities shift to the higher magnetic field region with increasing tilt angle θ of the applied magnetic field and the variation of peak position increases as the tilt angle θ of the applied magnetic field increases. (iv) The splitting of the ODMPR peaks takes place from MPR peaks and the width of splitting depends on the incident photon frequency. The splitting width from MPR peaks increases with increasing incident photon frequency. (v) The height of these peaks in the conductivities are closely related to the tilt angle θ. The height of these peaks increases with increasing tilt angle θ of the applied magnetic field. The resonant behaviors are actually given by $P\hbar\omega_s\pm\hbar\omega=\hbar\omega_{LO}(P\equiv N'-N=1$, 2, and 3). If there is no photon energy $\hbar\omega$ in the ODMPR condition, it becomes MPR condition given by $P\hbar\omega_s=\hbar\omega_{LO}(P\equiv N'-N=1,2,3)$. Accordingly we see that the ODMPR peaks are split from the MPR peaks. It seems that the splitting is due to the absorption and emission of a photon during the absorption of a phonon.

Figures 2(a), 2(b), and 2(c) show the magnetic-field strength dependence of the magnetoconductivities $\overline{\sigma_{yy}}(\overline{\omega})$ as a function of photon frequency for the various tilt angles θ in case of $\omega/\omega_{LO}=1.0,0.7$, and 0.4 at $T=250$ K. Various peaks are observed according to the incident photon frequency and the strength of magnetic field. It is clearly seen from the figures that main peaks are observed in terms of the cyclotron resonance condition $(\omega=\omega_c)$, whereas subsidiary peaks are exhibited in terms of the ODMPR condition $(P\hbar\omega_s\pm\hbar\omega=\hbar\omega_{LO})$. As the tilt angle θ of the applied magnetic field increases, the peaks due to the ODMPR shift to the smaller value region of ω/ω_{LO}. As the value of ω_c/ω_{LO}

decreases, the number of the resonant peaks increase. Therefore, all peaks can be assigned from the cyclotron resonance (CR) and the ODMPR condition.

Figures 3(a) and 3(b) show the magnetic field strength dependence of the magnetoconductivities $\overline{\sigma_{yy}}(\overline{\omega})$ as a function of photon frequency for the various temperature in the cases of $\omega/\omega_{LO}=1.0$, and 0.4 at $\theta=0°$, 30°, and 70°, respectively. Various peaks are observed according to the incident photon frequency and the strength of magnetic field as those in Figs. 2(a), 2(b), and 2(c). As the temperature increases, the height of these peaks due to the ODMPR decreases at the fixed values region of ω/ω_{LO}. As the value of ω_c/ω_{LO} decreases and the tilt angle θ of the applied magnetic field increases, the number of the resonant peaks increase as those in Figs. 2(a), 2(b), and 2(c).

Figures 4(a), 4(b), and 4(c) show the shifts of resonant peaks as a function of tilt angle θ of the applied magnetic field for the various P values in case of $\omega=0$, 3, and 7 THz. The shifts of resonant peaks are observed according to the incident photon frequency and the P values as a function of tilt angle of the applied magnetic fields. The shifts of resonant peaks are the largest at 90° tilted angle for all of the incident photon frequencies and the P values. The splitting of the shifts of resonant peaks increases with increasing photon frequency like those in Figs. 1 and 2.

So far, we have applied the angular dependent magnetoconductivity $\overline{\sigma_{yy}}(\overline{\omega})$ obtained by using the Mori-type projection operator technique to n-Ge materials and studied the anomalous behavior of the ODMPR line shape, such as the splitting and the shift of ODMPR of the angular dependent magnetoconductivity $\overline{\sigma_{yy}}(\overline{\omega})$.

Our results show the following. (1) As a linearly polarized photon of amplitude E and frequency ω is incident along the z axis, the splitting of the ODMPR peaks takes place from the MPR peaks. (2) As the photon frequency is increased, the shifts of the ODMPR peak positions are increased. (3) As the difference of Landau level indices is increased, the MPR and ODMPR peak positions are shifted to the lower magnetic field side and the shifts of ODMPR is decreased. (4) The peaks in the magnetoconductivities shift to the higher magnetic field region with increasing tilt angle θ of the applied magnetic field and the variation of peak position increases as the tilt angle θ of the applied magnetic field increases. (5) The splitting width from MPR peaks increases with increasing incident photon frequency. (6) The height of these peaks increases with increasing tilt angle θ of the applied magnetic field. (7) As the tilt angles θ of the applied magnetic field increases, the peaks due to the ODMPR shift to the smaller value region of ω/ω_{LO}. (8) As the value of ω_c/ω_{LO} decreases, the number of the resonant peaks increase. (9) As the temperature increases, the height of these peaks due to the ODMPR decreases at the fixed values region of ω/ω_{LO}. (10) The shifts of resonant peaks are the largest at 90° tilted angle for all of the incident photon frequencies and the difference of Landau indices values. In addition, strong oscillations of the magnetoconductivity in bulk materials such as n-Ge are expected in terms of the optically detected magnetophonon resonance, which indicate that the ODMPR should also be observed experimentally in such bulk semiconductors, as pointed out by Hai and Peeters.[8] Despite the above shortcomings of the theory, we believe that our results make it possible to understand analytically the essential physics of ODMPR in nonpolar materials.

This work was supported by the Korea Research Foundation Grant No. KRF-2001-037-DA0015.

[1] V. L. Gurevich and Yu. A. Firsov, Zh. Éksp. Teor. Fiz. **40**, 198 (1961) [Sov. Phys. JETP **13**, 137 (1961)].
[2] R. J. Nicholas, Prog. Quantum Electron. **10**, 1 (1985).
[3] D. Schneider, C. Brink, G. Irmer, and P. Verma, Physica B **256-258**, 625 (1998); D. Schneider, K. Pricke, J. Schulz, G. Irmer, and M. Wenzel, in *Proceedings of the 23rd International Conference on the Physics of Semiconductors*, edited by M. Scheffler and R. Zimmermann (World Scientific, Singapore, 1996), p. 221.
[4] N. Mori, H. Momose, and Hamaguchi, Phys. Rev. B **45**, 4536 (1992).
[5] J. Y. Ryu and R. F. O'Connell, Phys. Rev. B **48**, 9126 (1993); J. Y. Ryu, G. Y. Hu, and R. F. O'Connell, *ibid.* **49**, 10 437 (1994).
[6] A. Suzuki and M. Ogawa, J. Phys. C **10**, 4659 (1998).
[7] S. C. Lee, J. Y. Ryu, S. W. Kim, and C. S. Ting, Phys. Rev. B **62**, 5045 (2000); S. Y. Choi, S. C. Lee, H. J. Lee, H. S. Ahn, S. W. Kim, and J. Y. Ryu, Phys. Rev. B **66**, 155208 (2002).
[8] G.-Q. Hai and F. M. Peeters, Phys. Rev. B **60**, 16 513 (1999).
[9] J. Y. Ryu, Y. C. Chung, and S. D. Choi, Phys. Rev. B **32**, 7769 (1985); J. Y. Ryu and S. D. Choi, Prog. Theor. Phys. **72**, 429 (1984).
[10] S. D. Choi and O. H. Chung, Solid State Commun. **46**, 717 (1983).
[11] J. Singh, *Physics of Semiconductors and their Heterostructures* (McGraw-Hill, Singapore, 1993), p. 455.
[12] B. K. Ridley, *Quantum Processes in Semiconductors* (Clarendon Press, Oxford, 1993), p. 256.